

Robotic Cutting of Solids Based on Fracture Mechanics and FEM

Prajjwal Jamdagni and Yan-Bin Jia

Abstract—Cutting skills are important for robots to acquire not only because of a need from kitchen automation, but also because of the technical challenge for robotic manipulation. Modeling of fracture and deformation during a cutting action, often based on the finite element method (FEM), provides the force and shape information used in knife control to implement a skill such as slice, chop, or dice. However, an object’s 3D mesh model can be computationally prohibitive for achieving a desired accuracy since numerous tiny elements must be used near the knife’s moving edge. To address this issue, we represent the object as evenly spaced slices normal to the cutting plane such that cutting of each slice requires only a 2D mesh. Fracture and force can be then interpolated between every two adjacent slices. Experiment with an Adept arm and an ATI force/torque (F/T) sensor has demonstrated reasonable accuracy in force and shape modeling.

I. INTRODUCTION

Fruits, vegetables, and meat are vital food resources in our life. They are often non-uniform and deformable, sometimes slippery, and other times textured. A big challenge faced by a robot in the kitchen is how to cut natural foods with basic skills such as chop, slice, and dice. To cut an object, the robot must control the knife to generate fracture, overcome friction and viscosity, and comply to various task constraints.

Control policies for cutting need to be developed based on different requirements and even during periods of a single cutting action, which often consists of multiple movements [1]. Different movements, such as pressing the knife downward and slicing via moving its edge on the cutting board, requires knowledge of different forces. However, force data sensed while cutting combines forces from different origins including deformation, fracture, contact, and friction (both knife-object and knife-board). Among them, the fracture force directly affects the progress of cutting, while the contact force maintains an environmental constraint. Separation of forces of different nature mashed in the sensor readings is possible via modeling of cutting, which is also important for planning as it can predict the outcome of a potential cutting trajectory or the events ahead along the current trajectory so adjustments can be made in time.

Modeling of fracture [2] is based on a balance between the work performed by the knife and the sum of the portion

responsible for fracture, the strain energy stored/released due to deformation, the amount of energy dissipated through friction, etc. As cutting lasts over a short time period, modeling bears an incremental nature to track the varying crack and shape of the object. Meanwhile, the nature of the process makes the finite element method (FEM) a very good choice for modeling.

FEM-based modeling may proceed iteratively as follows. Within each iteration, the knife moves downward for a very small distance, conducting extra work. If the crack propagates, it will release some strain energy of an amount that in turn depends upon the length of the new crack. The crack propagates when this energy release rate exceeds the material property *fracture toughness*. Meanwhile, we predict the force component that propagates the crack, as well as the component that overcomes friction.

Carrying out the above simulation over a 3D mesh model can be computationally prohibitive as tiny elements have to be used near the knife’s edge for good accuracy ($\approx 10^6$ elements). Instead we will represent the object as a sequence of evenly spaced cross sections perpendicular to the cutting plane. Each cross section is represented by a 2D mesh, which affords the use of tiny elements ($\approx 10^4$ elements). Interpolation is applied between every two adjacent slices to complete modeling of the object. Boundary conditions on the hanging portions of the 2D slices are obtained using a separate FEM carried out on a coarse 3D mesh model of the object.

This paper focuses on modeling how an object fractures and deforms as it is being cut by a knife attached to a robotic arm. Section II describes some related works from fracture mechanics, machining, cutting of biological tissues, and control of robotic cutting. Section III reduces the 3D modeling task to multiple 2D modeling tasks, each solvable via the same FEM procedure and together with their modeling results interpolated. Section IV shows experiment conducted over five food items to demonstrate good matches between the modeled force, torque, and work experienced by the knife, and the measurements by a six-axis force/torque sensor. Section V outlines some future extensions to the presented work.

A vector is represented by a lowercase letter in bold, e.g., $\mathbf{p} = (p_x, p_y)^T$, with its x - and y -coordinates denoted by the same (non-bold) letter with subscripts x and y , respectively. A matrix is represented by an uppercase letter in bold, e.g., \mathbf{K} . The SI units are used throughout the paper.

*Support for this research has been provided by the US National Science Foundation under Grant IIS-1651792. Any opinions, findings, and conclusions or recommendations expressed in this material are those of the authors and do not necessarily reflect the views of the National Science Foundation.

*We would like to thank Xiaoqian Mu and Yuechuan Xue for their early help with the experiments. We also thank anonymous reviewers for their valuable feedback.

The authors are with the Department of Computer Science, Iowa State University, Ames, IA 50011, USA prajjwal, jia@iastate.edu

II. RELATED WORK

A comprehensive survey [3] presented basic mechanics of cutting and compared different models used for fracturing soft tissues and bones. Fracture toughness was estimated for ductile materials [4] in cutting and for organ tissues in needle insertion [5], [6], of which mechanics were empirically investigated in [7]. Analyses of stress and fracture force [8]–[10] for cutting bio-materials accounted for factors including blade sharpness and slicing angle. The “slice/push ratio” introduced in [11] characterizes the dramatic force decrease as a result of the knife’s “pressing and slicing”. For flexible solids that undergo negligible deformation during cutting, this ratio was employed to conveniently compute the cutting force and torque via an integration along the edge of the blade [12].

FEM was used to simulate machining by checking the shear stress ahead of the tool tip to determine chip separation [13], to detect crack propagation based on the stress intensity factor and the J -integral [14], and to calculate energy release rate at the crack front using virtual crack extension [15]. To cut down the computational cost, extended FEM (XFEM) was developed to model discontinuities like fracture, dislocation and phase interfaces [16], and crack propagation [17] without remeshing. Recently, phase-field model [18] for crack growth has been proposed for accurate modeling of continuous crack evolution using a damage parameter. In our modeling task, we cannot avoid remeshing because the contact between knife’s edge and crack front needs to be represented with enough accuracy for reliable force estimation. In [19], simulation and experiment with soft tissues were conducted based on FEM modeling of deformations to determine cutting parameters in a computationally efficient way. Given their complicated mechanical behaviors, cutting of soft tissues are more accurately modeled using the nonlinear FEM, as in the work [20] which also applied element separation and node snapping to create a cut.

Measurements from food cutting revealed that the cutting force and friction will decrease when the temperature increases, or when the speed decreases [21]. Moisture content and storage period were found to affect the physico-mechanical properties of food [22]–[26].

Adaptive control was applied to learn the cutting force from the histories of position and velocity [27], impedance control was employed to track such force [28], and also to implement the cooperation of two robots on trajectory following and object stabilization [29]. Force control and visual servoing were combined to implement multiple cuts along a specified trajectory to cope with modeling errors and environment constraints [30].

III. MODELING

The aim of our FEM-based modeling is to predict the force response and deformation of a solid being cut by a knife. As shown in Fig. 1(a), we align the xz -plane with the top surface of the cutting board. The knife, whose plane of symmetry coincides with the xy -plane, is translating in the negative y -direction. We make the following assumptions:

1. the object is isotropic and linearly elastic;
2. it remains stable during cutting;
3. the action of cutting is quasi-static;
4. the fracture is generated in the yz -plane only;
5. the linear elastic fracture mechanics is applicable;
6. during the cutting every cross section of the object parallel to the xy -plane will stay within its own plane.

Assumption 6 implies that every such cross section is in plane strain.¹ This assumption is reasonable since the knife’s edge applies force on a very narrow region of each cross section, which is constrained on both sides by large mass, and a state of plane strain exists along most of the crack tip [31].

In a 3D mesh model of the object, very small elements would have to be used near the knife’s edge. The computational cost can become extremely high to achieve even a moderate accuracy. Instead, we will use 2D meshes to represent a number of evenly spaced cross sections that are parallel to the xy -plane. Generally, the object’s cross

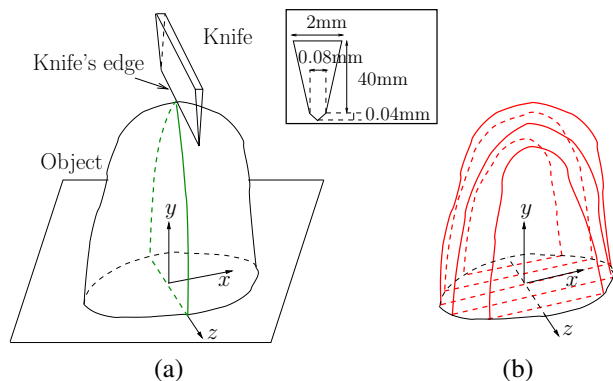


Fig. 1: (a) Cutting in the yz -plane. (b) Object represented by evenly spaced slices parallel to the xy -plane. Inset shows the geometry of a cross section of the knife’s blade that is parallel to the xy -plane.

section may vary continuously along the z -axis as shown in Fig. 1(b). We consider evenly spaced cross sections along the z -axis, and focus on one of them, say, S , without loss of generality. We will present how to model cutting of S . Then, we will model cutting of the entire object via interpolating the behaviors of individual cross sections.

A. Cutting a Cross Section

The cross section S is meshed using triangular elements, as shown in Fig. 2a. The knife’s cross section, coplanar with S , is symmetric with respect to the y -axis. On the top right of the figure, the gray dots are the nodes in contact with either side of the knife’s blade, and the black dots are the nodes in contact with its edge. Smaller elements are near the edge to accurately model fracture, whereas larger elements are away from the knife to keep the total number low.

We also create a special zone surrounding the y -axis (i.e., the cutting line) called the *separation layer*. This thin layer, one element wide on each side of the y -axis, is used for simulating crack propagation illustrated in Fig. 3.

¹For very thin objects this assumption may lead to underestimation of the cutting force.

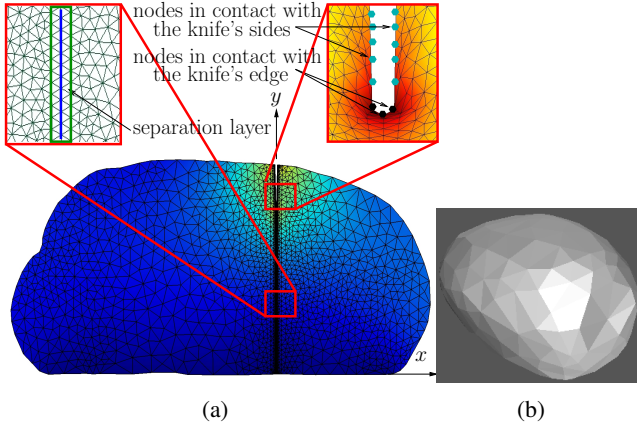


Fig. 2: (a) Cutting of a meshed cross section of a tomato downward along the y -axis. The enlarged rectangular area on the top left shows the separation layer (inside the green box) around the y -axis (blue). The enlarged area on the top right shows nodes in contact with the knife's edge and blade. (b) A surface mesh generated from laser scanner point cloud of the tomato.

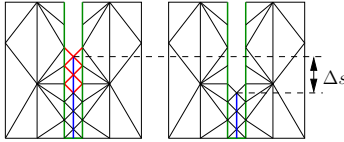


Fig. 3: Crack propagation. The green line segment bounds the separation layer, in which the elements are removed to extend the crack. The blue line segment lies on the y -axis.

We use the linear elastic fracture mechanics (LEFM) based on energy balance for modeling crack propagation. During the cutting plastic deformation occurs at the crack front before material fracture. Assumption 5 implies that this plastic deformation zone is very

small compared to the object's dimensions, and its position remains constant relative to the crack front throughout the cutting process. LEFM approximates energy exchange during crack propagation (plastic deformation, new surface generation etc.) using a material property *fracture toughness*, R_c , which is defined as the energy required to extend fracture by unit area. The term R_c is a material constant under Assumption 5.

Let $F(z)$ be the density of force on the object along the z -axis, i.e., the force exerted on its cross section at the position determined by the value of z . Similarly, let the densities $U(z)$ and $W(z)$ respectively represent the strain energy of the same cross section and the work done by the knife on it. Neglecting friction, the following equation describes the energy balance during continuous cutting when the crack is extended downward by an infinitesimal length ds for an infinitesimal work dW by the knife [2],

$$dW = 2R_c ds + dU \quad (1)$$

The energy required for crack propagation is provided in part by the knife, and in part by release of strain energy. The *energy release rate* is defined as $R = (dW - dU)/2ds$. According to LEFM the crack propagates when $R \geq R_c$. Because U is a function of the crack length, object geometry, and force loading, equation (1) does not have a closed-form solution for a general object. We simulate the continuous

cutting phase iteratively based on the FEM as follows.

In each iteration the knife moves downward until the crack propagates. Let \mathbf{f} be the vector of nodal forces, $\Delta\mathbf{b}$ be the vector of nodal displacements, and \mathbf{K} be the stiffness matrix. At the start of the i th iteration, the knife's edge is currently at the position $y = y_i$, and we know the corresponding values \mathbf{f}_i , $\Delta\mathbf{b}_i$, and \mathbf{K}_i . The strain energy subsequently is $U_i = \frac{1}{2}\Delta\mathbf{b}_i^T \mathbf{K}_i \Delta\mathbf{b}_i$. Within the iteration, the knife's edge moves from the current position y_i to a new position $y_{i+1} = y_i + \epsilon$, for some constant $\epsilon < 0$. First, assuming no new fracture (and thus using the same mesh), we calculate new values \mathbf{f}_{i+1} , $\Delta\mathbf{b}_{i+1}$, and U_{i+1} as will be described in Section III-B. The work done by the knife would then be $\Delta W = U_{i+1} - U_i$. Keeping the knife at y_{i+1} , we create a new mesh with the crack extended by some small length $\Delta s = \delta$.² The updated force, displacement, and energy values are obtained as $\tilde{\mathbf{f}}_{i+1}$, $\tilde{\Delta\mathbf{b}}_{i+1}$, and \tilde{U}_{i+1} , respectively. A crack extension by Δs would release strain energy of the amount $\Delta U = \tilde{U}_{i+1} - U_i$, yielding the energy release rate of $R = (\Delta W - \Delta U)/(2\Delta s)$. If $R < R_c$, then the amount of energy released due to crack propagation is insufficient. In this case, we repeatedly decrease y_{i+1} by ϵ until $R \geq R_c$ at $y_{i+1} = y_i + j\epsilon$ for some $j > 0$. If $R \geq R_c$, we find the value of the crack extension Δs such that

$$\Delta W = 2R_c \Delta s + \Delta U. \quad (2)$$

We solve equation (2) for Δs via bisection over the interval $[(k-1)\delta, k\delta]$ keeping the knife fixed at y_{i+1} .³

To extend the crack downward by Δs , we find the node on the y -axis that is the closest to the tip's new position in the undeformed mesh. Then we remove all the elements within the separation layer that are above this position (see Fig. 3).

Sometimes the object has a skin that is tougher to cut than the interior of its body. To cope with this, we use two different values for fracture toughness. A higher one is used for the skin before crack happens, and a lower one is used for the interior afterwards. Table I in Section IV lists the fracture toughness for different objects used in the experiment.

B. Knife Force and Object Deformation

To solve for the force exerted by the knife, we need to apply two types of boundary conditions. A condition of the first type restricts a contact node between the object and the cutting board on the x -axis to move along the axis only, or a node in the xz -plane to stay in the plane. Additionally, some nodes in the xz -plane may be fixed due to friction between the object and the cutting board. Let $\mathbf{p} = (p_x, p_y)^T$ and $\mathbf{u} = (u_x, u_y)^T$ be the position and displacement of a node respectively. If \mathbf{p} is of the first type, then it satisfies one or both of the following: $u_y = 0$ and $u_x = 0$.

A boundary condition of the second type is exerted on a contact node between the knife and the object. The contact is with either the knife's edge or its blade. In the first case (shown as a black dot on the upper right in Fig. 2a) the

²The value of δ can be determined, for instance, by the size of the smallest mesh element.

³The initial value of k is 2, which can be increased if required.

node is assumed to stick to the edge and thus moves with it in the y -direction only. If this is the case with \mathbf{p} , then its displacement \mathbf{u} satisfies $u_x = 0$ and $u_y = h - p_y$, where h is the height of knife's edge above the xz -plane. In the second case, every node in contact with one side of the blade only moves on that side and in the cross section (parallel to the xy -plane). As the side of knife is represented by a line in 2D, the displacement for such node satisfies the equation $a(p_x + u_x) + b(p_y + u_y) + c = 0$, where a , b , and c are coefficients of the intersection line of the side of the blade with the xy -plane.

Let m be the number of constraints, and n be the mesh's total number of degrees of freedom. All the constraints can be combined into an equation $\mathbf{A}\mathbf{u} = \mathbf{b}$, where \mathbf{A} is an $m \times n$ matrix. Applying the above constraints, we minimize the following Lagrangian

$$L(\mathbf{u}, \boldsymbol{\lambda}) = \frac{1}{2} \mathbf{u}^T \mathbf{K} \mathbf{u} - \mathbf{u}^T \mathbf{f} + \boldsymbol{\lambda}^T (\mathbf{A} \mathbf{u} - \mathbf{b})$$

where $\boldsymbol{\lambda}$ is a vector of multipliers. This yields the following first order necessary condition:

$$\begin{bmatrix} \mathbf{K} & \mathbf{A}^T \\ \mathbf{A} & \mathbf{0} \end{bmatrix} \begin{bmatrix} \mathbf{u} \\ \boldsymbol{\lambda} \end{bmatrix} = \begin{bmatrix} \mathbf{f} \\ \mathbf{b} \end{bmatrix}$$

which can be solved for the deformation \mathbf{u} and $\boldsymbol{\lambda}$. The total force exerted by the knife and cutting board can be recovered as $-\mathbf{A}^T \boldsymbol{\lambda}$.

C. Interpolating Between Two Cross Sections

Let the function $\mathbf{f}(y, z)$ describe the density of the force at the knife's edge when it is at the height y inside the object's cross section at the distance z from the xy -plane. Carrying out the procedure in Sections III-A and III-B, we obtain the values of \mathbf{f} for discrete heights y_i and cross section locations z_j . The following polynomial, constructed through fitting, is used to describe the force density profile for the j th cross section:

$$\mathbf{f}(y, z_j) = a_{j,k} y^k + a_{j,k-1} y^{k-1} + \dots + a_{j,1} y^1 + a_{j,0}$$

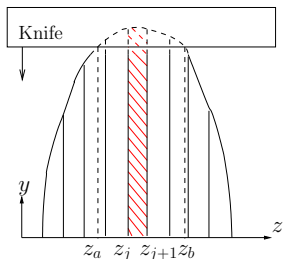


Fig. 4: Force exerted by the knife via interpolation and integration.

at the position z , $z_j < z < z_{j+1}$:

$$\mathbf{f}(y, z) = \frac{z - z_j}{z_{j+1} - z_j} \mathbf{f}(y, z_j) + \frac{z_{j+1} - z}{z_{j+1} - z_j} \mathbf{f}(y, z_{j+1}) \quad (3)$$

The total force by the knife when its edge is at the height y can be obtained via integrating (3) along the knife edge: $\mathbf{f}(y) = \int_{z_a}^{z_b} \mathbf{f}(y, z) dz$, where z_a and z_b determine the

segment of contact between the knife's edge and the object (see Fig. 4).

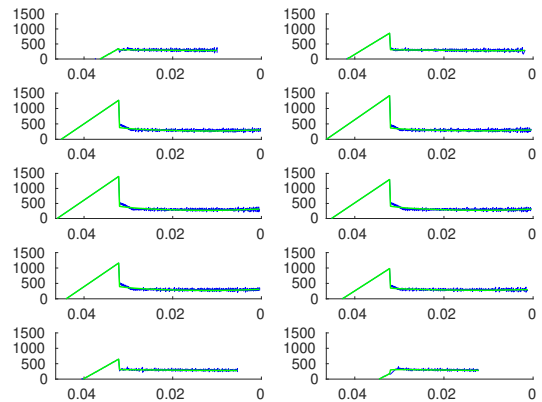


Fig. 5: Force per unit length (ordinate) vs knife height (abscissa) for the chosen cross sections of the mesh in Fig. 2b (left to right and top-down) in the increasing order of the z -coordinate with a fixed increment of 4.62mm.

D. Combining With Coarse 3D FEM

So far we have assumed that all the cross sections are independent of each other, and in contact with the cutting board (and thus constrained by it). For many objects this may not be true. Such an object may have “hanging” cross sections, which are not in contact with the cutting board but constrained by the body material on each side. To obtain boundary conditions for these cross sections, we construct a separate 3D mesh with a crack at the same location obtained from 2D simulation. The deformation of this coarse mesh at the current knife position yields good estimates for the x and y displacements of the boundary nodes of the hanging cross sections via interpolation.

E. Simulation Algorithm

At the start, the knife is positioned above the object. For each of its small downward movement, we carry out the 2D simulation procedure on selected cross sections as described in Sections III-A through III-C to propagate crack and determine the fracture and friction forces. After every few incremental knife movements, we call upon the coarse 3D simulation to update boundary conditions for the hanging portions of the cross sections. Interpolation is performed over all the cross sections to determine the overall deformation, fracture, and forces of fracture and friction.

IV. EXPERIMENT

An experiment was conducted with an ADEPT Cobra 800 robot to which a kitchen knife was rigidly attached. In between was a 6-axis F/T sensor (Delta IP65) from ATI Industrial Automation was mounted. As shown in the Fig. 7, an object was placed on a wooden board below the knife. A laser scanner was used to obtain a point cloud of the object, which was then processed using the *CGAL* open source library to generate a surface mesh (see Fig. 2b).

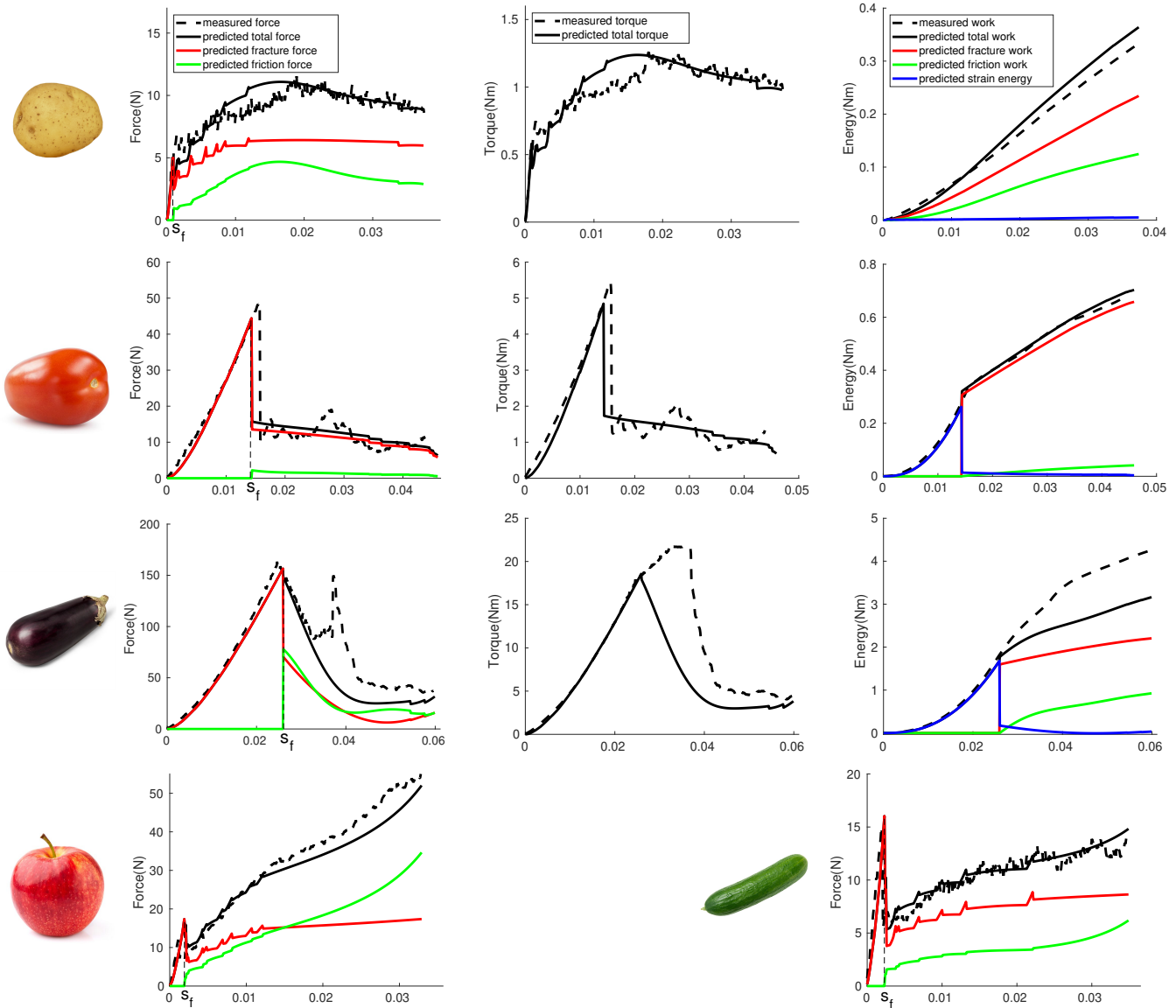


Fig. 6: Comparison of experimental and simulation results from cutting a potato, tomato, eggplant, apple and cucumber. The horizontal axis is knife displacement in the downward y -direction. Fracture happens at the depth s_f for each cutting.

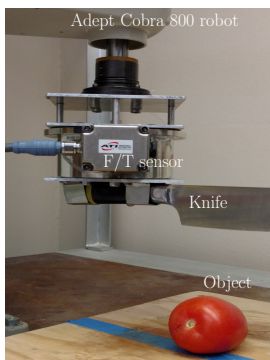


Fig. 7: Experimental setup.

Next, the mesh was intersected vertically by ten parallel and evenly spaced planes to generate cross sections used for modeling. Open source software *GMSH* was used to generate a mesh for each cross section. The robot translated the knife downward at the speed of 0.00625m/s. Modeling of the cutting of each cross section was carried out as described in Sections III-A through III-C using the open source library *Getfem++*.

A potato, an apple, a cucumber (no seeds), a tomato, and an eggplant were used. Table I lists the mechanical

TABLE I: Mechanical properties of five objects in the experiment: Young's modulus (E), Poisson's ratio (ν), coefficient of blade-material friction (μ), interior fracture toughness (R_c), and skin fracture toughness (R'_c).

Object	E (N/m)	ν	μ	R_c (N/m)	R'_c (N/m)
Potato	2×10^6	0.45	0.6	75	160
Apple	3×10^6	0.17	0.6	150	400
Eggplant	0.55×10^6	0.16	1.0	130	900
Tomato	0.4×10^6	0.3	0.18	130	400
Cucumber	2.5×10^6	0.37	0.5	125	450

properties of the five foods.⁴ Since the value of E is affected by moisture and the time of storage, we tuned it slightly based on the initial slope of force-displacement curve before fracture occurs

All the foods had been manually cut beforehand to provide

⁴Young's modulus (E) and Poisson's ratio (ν) for different foods were measured as considered in [22]-[26].

a flat base to sit on the cutting board. Friction between the board and such an object together with the constraint imposed by the knife were sufficient to prevent any rigid body motion. Based on our model, we predicted the force, torque, and work (product of R_c and the crack area) done due to fracture, friction, and strain energy. Fig. 6 compares the values of force, torque, and work during cutting from simulation and measured in the experiment. The cutting force and torque for all the objects were predicted quite well before fracture occurred at the depth s_f . The potato, apple, and cucumber were harder than the tomato and eggplant, deformed less, and fractured much earlier. The force required for initiating a crack was high compared to that for propagating the crack because of the tougher skin for all the foods.

The predicted forces after occurrence of fracture also closely followed the measured values for all the foods except the eggplant. The latter object's large deformation and tough skin had resulted in an uneven crack initiation across the knife's edge. Because of this, the measured force decreased, and the torque increased due to the changing point of application by the resultant force. The third plot in each of the first three rows shows a good match between the predicted and measured values of the work performed.

V. FUTURE WORK

Most food materials are not linear isotropic solids. Also the assumption about fracture only in the cutting plane is hardly true for very soft objects. Better force and deformation predictions can be done by removing these assumptions. We consider cutting by pressing only which is not an efficient method for cutting. We plan to consider slicing as well in the future. For very soft objects we would also like to track evolution of contact on the blade as individual area elements may switch between the contact modes of slip and stick under friction.

REFERENCES

- [1] X. Mu, Y. Xue, Y.-B. Jia. "Robotic cutting: Mechanics and control of knife motion," in *Proc. IEEE Int. Conf. Robot. Autom.*, 2019, in press.
- [2] T. Atkins. *The Science and Engineering of Cutting*. Elsevier, Oxford OX2 8DP, UK, 2009.
- [3] B. Takabi and B. L. Tai. "A review of cutting mechanics and modeling techniques for biological materials," *Medical Engr. Phys.*, 45:1-14, 2017.
- [4] A. G. Atkins. "Toughness and cutting: a new way of simultaneously determining ductile fracture toughness and strength," *Engr. Fracture Mechanics*, vol. 72, pp. 850-860, 2004.
- [5] C. Gokgol, C. Basdogan, and D. Canadinc. "Estimation of fracture toughness of liver tissue: Experiments and validation," *Medical Engr. Phys.*, vol. 34, pp. 882-891, 2012.
- [6] T. Azar and V. Hayward. "Estimation of the fracture toughness of soft tissue from needle insertion," in *LNCIS*, Springer-Verlag Berlin, 2008, pp. 166-175.
- [7] M. Khadem, C. Rossa, R. S. Sloboda, N. Usmani, and M. Tavakoli. "Mechanics of tissue cutting during needle insertion in biological tissue," *IEEE Robot. Autom. Letters*, vol. 1, no. 2, pp. 800-807, 2016.
- [8] D. Zhou, M. R. Claffee, K.-M. Lee, and G. V. McMurray. "Cutting, 'by pressing and slicing', applied to robotic cutting bio-materials, Part I: Modeling of stress distribution," in *Proc. IEEE/RSJ Int. Conf. Intell. Robots Syst.*, 2016, pp. 2896-2901.

- [9] D. Zhou, M. R. Claffee, K.-M. Lee, and G. V. McMurray. "Cutting, 'by pressing and slicing', applied to robotic cutting bio-materials, Part II: Force during slicing and pressing cuts," in *Proc. IEEE/RSJ Int. Conf. Intell. Robots Syst.*, 2006, pp. 2256-2261.
- [10] D. Zhou and G. McMurray. "Modeling of blade sharpness and compression cut of biomaterials," *Robotica*, vol. 28, pp. 311-319, 2010.
- [11] A. G. Atkins, X. Xu, and G. Jeronimidis. "Cutting, by 'pressing and slicing,' of thin floppy slices of materials illustrated by experiments on cheddar cheese and salami," *J. Materials Sci.*, vol. 39, pp. 2761-2766, 2004.
- [12] A. G. Atkins and Xianzhong Xu. "Slicing of soft flexible solids with industrial applications," *Int. J. Mech. Sci.*, vol. 47, pp. 479-492, 2005.
- [13] J. M. Huang and J. T. Black. "An evaluation of chip separation criteria for the FEM simulation of machining," *ASME J. Manufacturing Sci. Engr.*, vol. 118, pp. 545-554, 1996.
- [14] S. K. Chan, I. S. Tuba, W. K. Wilson. "On the finite element method in linear fracture mechanics," in *Engineering Fracture Mechanics*, vol. 2, pp. 1-17, 1970.
- [15] H. G. Delorenzi. "Energy release rate calculations by the finite element method," in *Engineering Fracture Mechanics*, vol. 21, pp. 129-143, 1985.
- [16] T.-P. Fries, T. Belytschko. "The extended/generalized finite element method: An overview of the method and its applications," *Int. J. Numer. Meth. Engr.*, vol. 84, pp. 253-304, 2010.
- [17] N. Moes, J. Dolbow, T. Belytschko. "A finite element method for crack growth without remeshing," *Int. J. Numer. Meth. Engr.*, vol. 46, pp. 131-150, 1999.
- [18] M. J. Borden, T. J. R. Hughes, C. M. Landis, A. Anvari, I. J. Lee. "A phase-field formulation for fracture in ductile materials: Finite deformation balance law derivation, plastic degradation, and stress triaxiality effects," *Comp. Meths. Applied Mech. Engr.*, vol. 312, pp. 130-166, 2016.
- [19] T. Chanthasopeephan, J. P. Desai, and A. C. W. Lau. "Modeling soft-tissue deformation prior to cutting for surgical simulation: Finite analysis and study of cutting parameters," *IEEE Trans. Biomed. Engr.*, vol. 54, no. 3, pp. 349-359, 2007.
- [20] B. Ghali and S. Sirouspour. "Nonlinear finite element-based modeling of soft-tissue cutting," in *Proc. IEEE Toronto Int. Conf. Sci. Tech. Humanity*, 2009, pp. 141-146.
- [21] T. Brown, S. J. James, and G. L. Purnell. "Cutting forces in foods: experimental measurements," *J. Food Engr.*, vol. 70, pp. 165-170, 2005.
- [22] O. Kabas, A. Ozmerzi. "Determining the mechanical properties of cherry tomato varieties for handling," in *J. Texture Studies*, vol. 39, pp. 199-209, 2008.
- [23] M. Bentini, C. Caprara, R. Martelli. "Physico-mechanical properties of potato tubers during cold storage," in *Biosystems Engineering*, vol. 104, pp. 25-32, 2009.
- [24] M. Grotte, F. Duprat, E. Pietri, D. Loonis. "Young's modulus, Poisson's ratio and Lamé's coefficients of golden delicious apple," in *Int. J. Food Properties*, vol. 5, pp. 333-349, 2002.
- [25] S.M. Ashtiani, M.R. Golzarian, J.B. Motie, B. Emadi, N.N. Jamal, H. Mohammadinezhad. "Effect of loading position and storage duration on the textural properties of eggplant," in *Int. J. Food Properties*, vol. 19, pp. 814-825, 2016.
- [26] O. Eboibi, H. Uguru. "Effect of moisture content on the mechanical properties of cucumber fruit," in *Int. J. Sci. Engr. Research*, vol. 9, pp. 671-678, 2018.
- [27] G. Zeng and A. Hemami. "An adaptive control strategy for robotic cutting," in *Proc. IEEE Int. Conf. Robot. Autom.*, 1997, pp. 22-27.
- [28] S. Jung and T. C. Hsia. "Adaptive force tracking impedance control of robot for cutting nonhomogeneous workpiece," in *Proc. IEEE Int. Conf. Robot. Autom.*, 1999, pp. 1800-1805.
- [29] P. Long, W. Khalil, and P. Martinet. "Modeling and control of a meat-cutting robotic cell," in *Proc. Int. Conf. Advanced Robot.*, 2013, pp. 61-66.
- [30] P. Long, W. Khalil, and P. Martinet. "Force/vision control for robotic cutting of soft materials," in *Proc. IEEE/RSJ Int. Conf. Intell. Robots Syst.*, 2014, pp. 4716-4721.
- [31] T. L. Anderson. *Fracture Mechanics: Fundamentals and Applications*. CRC Press, Boca Raton, FL 33487-2742, US, 2005.